NeuroImage: Clinical 28 (2020) 102378

Contents lists available at ScienceDirect

NeuroImage: Clinical

journal homepage: www.elsevier.com/locate/ynicl

Multilayer MEG functional connectivity as a potential marker for suicidal thoughts in major depressive disorder

Allison C. Nugent[a,b,*], Elizabeth D. Ballard[b], Jessica R. Gilbert[b], Prejaas K. Tewarie[c], Matthew J. Brookes[c], Carlos A. Zarate Jr.[b]

[a] MEG Core Facility, National Institute of Mental Health, National Institutes of Health, Bethesda, MD 20892, USA
[b] Experimental Therapeutics and Pathophysiology Branch, National Institute of Mental Health, National Institutes of Health, Bethesda, MD 20892, USA
[c] Sir Peter Mansfield Imaging Centre, School of Physics and Astronomy, University of Nottingham, University Park, Nottingham NG7 2RD, UK

ARTICLE INFO

Keywords:
Magnetoencephalography
Connectivity
Suicide
Major depressive disorder
Frequency
Oscillation

ABSTRACT

Major depressive disorder (MDD) is highly heterogeneous in its clinical presentation. The present exploratory study used magnetoencephalography (MEG) to investigate electrophysiological intrinsic connectivity differences between healthy volunteers and unmedicated participants with treatment-resistant MDD. The study examined canonical frequency bands from delta through gamma. In addition to group comparisons, correlational studies were conducted to determine whether connectivity was related to five symptom factors: depressed mood, tension, negative cognition, suicidal thoughts, and amotivation. The MDD and healthy volunteer groups did not differ significantly at baseline when corrected across all frequencies and clusters, although evidence of generalized slowing in MDD was observed. Notably, however, electrophysiological connectivity was strongly related to suicidal thoughts, particularly as coupling of low frequency power fluctuations (delta and theta) with alpha and beta power. This analysis revealed hub areas underlying this symptom cluster, including left hippocampus, left anterior insula, and bilateral dorsolateral prefrontal cortex. No other symptom cluster demonstrated a relationship with neurophysiological connectivity, suggesting a specificity to these results as markers of suicidal ideation.

1. Introduction

Major depressive disorder (MDD) is a highly prevalent and potentially severe mood disorder resulting in significant morbidity and mortality worldwide and is associated with a worldwide estimated lifetime prevalence of suicide attempt of 31% (Dong et al., 2019). Although some neurobiological substrates for MDD have been identified across several decades of research (Drevets et al., 2008), a comprehensive picture of the pathophysiology of MDD remains unknown. An additional complication is that MDD is a highly heterogeneous disorder. A DSM-V diagnosis of MDD requires the presence of either depressed mood or anhedonia, plus at least five of seven additional symptoms (APA, 2013). Some of these symptoms are opposite in nature; for instance, either hypersomnia or insomnia may be present. Thus, any two individuals with MDD could potentially overlap on only one symptom. Recently, an NIMH Research Domain Criteria (RDoC) framework (Insel et al., 2010) emerged that conceptualizes mental illness as dysfunction on multiple functional dimensions. While neurobiological circuit deficits have been implicated in several of these domains, the translation of this into depressive phenotypes has thus far been unsuccessful.

To date, most neuroimaging studies examining neurobiological circuits or functional connectivity in MDD compared participants directly with healthy controls (HCs). Increasingly, studies reporting altered resting-state functional connectivity in MDD have converged on a triple-network model of dysfunction (Kaiser et al., 2015). This model posits that abnormalities within and between three core networks are responsible for the manifestations associated with neuropsychiatric disorders (Menon, 2011). The three core networks include: the default mode network (DMN), which is involved in interoceptive and self-referential processing (Sheline et al., 2009); the central executive network (CEN), which is involved in goal-directed behavior; and the salience network (SN), which is thought to control switching between the DMN and CEN. Several studies have now investigated these networks directly in individuals with MDD and revealed both within- and between-network alterations (Manoliu et al., 2013; Wang et al., 2020a, 2020b). In addition, meta-analyses found that emotional processing in MDD largely involved the three core networks (Hamilton et al., 2012; Groenewold et al., 2013). To our knowledge, only one study directly

* Corresponding author at: 10 Center Drive, MSC 1059, Bldg, 10, Rm. 4N242, Bethesda, MD 20892-1059, USA.
E-mail address: nugenta@nih.gov (A.C. Nugent).

https://doi.org/10.1016/j.nicl.2020.102378
Received 2 December 2019; Received in revised form 18 June 2020; Accepted 6 August 2020
Available online 08 August 2020

investigated the core networks using magnetoencephalography (MEG); that study found increased broadband connectivity within the CEN, as well as increased connectivity of the SN with both the CEN and DMN (Tian et al., 2019). While other studies observed connectivity differences in targeted regions (such as the subgenual anterior cingulate cortex (sgACC), the dorsolateral prefrontal cortex (DLPFC), the anterior insula (AI), and/or the amygdala), the diversity of methods used makes it difficult to synthesize the results (Wang et al., 2019; Nugent et al., 2015).

Rather than simply comparing MDD and HC participants, some studies have adopted a dimensional approach that attempts to determine whether biological subtypes of depression correlate with clinical features or vice versa. For example, functional magnetic resonance imaging (fMRI) studies have attempted to determine neurobiological correlates of the melancholic subtype of MDD (Workman et al., 2016; Guo et al., 2016; Hyett et al., 2015) and primarily found reduced functional connectivity. Recently, Drysdale and colleagues (Drysdale et al., 2017) used a data-driven clustering technique to separate individuals with MDD into neurophysiological subtypes, or 'biotypes', based on resting-state functional connectivity measured using fMRI. Four biotypes emerged, differentiated on the basis of two feature scores: an 'anhedonia-related' component and an 'anxiety-related' component. The primary limitation of this study was that the full connectivity profile was reduced to only those connections showing maximal correlations with clinical characteristics, biasing any resulting clusters to differentiate on the basis of behavioral phenotype. This issue was elegantly highlighted by Dinga and colleagues (Dinga et al., 2019), who demonstrated that these biotype clusters are not sufficiently stable to be truly predictive. Another study (Feder et al., 2017) applied cluster analyses to functional connectivity in a cohort of individuals with MDD, some of whom exhibited only mild symptomatology at the time of the scan. Only weakly separable subgroups were observed, and they primarily differed in overall severity and length of illness (Feder et al., 2017). Thus, the search for brain-based subtypes of MDD remains ongoing.

Several electroencephalography (EEG) studies have examined clinically defined depressive subtypes. One study demonstrated that individuals with melancholic MDD exhibited greater sgACC delta activity compared to non-melancholic MDD participants (Pizzagalli et al., 2004). A more recent study found abnormalities in alpha asymmetry in non-melancholic MDD participants, while melancholic participants did not differ from controls (Quinn et al., 2014). These results have not been replicated. Presently, we know of no MEG studies that have investigated differences related to depressive subtypes or symptom clusters. While an array of studies have used multi-scale network frameworks to analyze brain activity at multiple temporal or spectral scales simultaneously (see reviews in De Domenico, 2017; Betzel and Bassett, 2017), relatively few have used source-localized MEG data and amplitude envelope correlations (AECs), and none have examined MDD using AEC. In this context, a MEG technique that has been referred to as "multilayer" (Brookes et al., 2016) can be used to examine all frequencies—rather than just one band—as well as interactions between frequencies. In the original publication, this multilayer technique was used to compare research participants with schizophrenia to HCs and found a posterior alpha band network where the groups differed and where connection strengths correlated with illness severity (Brookes et al., 2016).

The present study used a multilayer analysis to investigate differences in MEG intrinsic connectivity between HCs and individuals with MDD, with a particular focus on the three core networks. The study also examined the relationship between MDD symptom clusters and functional connectivity metrics. As our connectivity metric, we specifically examined correlations between fluctuations in band-limited power (also known as AECs) in resting-state MEG data from research participants with MDD and HCs. While complex analyses of how the individual layers within multi-layer networks interact can be conducted using metrics from graph theory (Tewarie et al., 2016), this exploratory report is limited to straightforward parametric comparisons of connection strengths. We also avoided examining differences in topological properties, as the procedures required to create sparse networks may be biased due to group differences in link density or average connectivity (Mandke et al., 2018). Finally, because our sample size was relatively small, any attempt to cluster participants into biotypes would be statistically untenable; therefore, we relied on a previously reported exploratory factor analysis (Ballard et al., 2018) that examined symptom clustering in a larger group of MDD participants. We then determined whether these clinical domains were associated with MEG functional connectivity. Given the dearth of published literature on resting-state MEG functional connectivity in MDD, this analysis was exploratory and the findings should be considered preliminary and hypothesis-generating. Nevertheless, based on previous fMRI (Evans et al., 2018; Greicius et al., 2007) and MEG (Nugent et al., 2015) findings, we hypothesized that abnormalities in connectivity would be observed in key nodes of the three core networks, including the sgACC, limbic regions, and AI.

2. Material and methods

2.1. Participants

Data from 29 male and female participants with MDD and 25 HCs were included in the present study. All participants were enrolled in a clinical trial (NCT00088699); participant characteristics and baseline differences in oscillatory gamma power for an overlapping group of the same participants has previously been published (Nugent et al., 2019). However, due to the use of ICA data cleaning, the present study was able to include additional participants who were not in the prior study (which included 24 MDD and 22 HC participants for the baseline session). Diagnoses were established using the Structured Clinical Interview for DSM-IV-TR (SCID) and an unstructured interview with a study psychiatrist. Participants were considered to be treatment-resistant, as defined by a history of non-response to at least one adequate antidepressant trial during their current episode, as assessed by the Antidepressant Treatment History Form (Sackeim, 2001). All participants had been free of any medications (both chronically and intermittently dosed) with potential neurological or psychotropic effects for at least two weeks (five weeks for fluoxetine). Participants with MDD were allowed psychiatric comorbidities provided that MDD was the primary diagnosis.

HCs had no Axis I disorder as determined by the SCID-NP and no family history of any Axis I disorder in first-degree relatives. Both MDD participants and HCs were in good physical health, as determined by medical history, physical exam, blood test results, electrocardiogram, chest x-ray, urinalysis, and toxicology screening. The study was approved by the National Institutes of Health (NIH) Combined Neuroscience Institutional Review Board, and all participants gave written informed consent before entry into the study.

2.2. Rating scale scores

Depressive symptoms for MDD participants were assessed using the Montgomery-Asberg Depression Rating Scale (MADRS) as the primary outcome measure of the clinical trial (Montgomery and Åsberg, 1979) at time points previously described (Nugent et al., 2019). The Beck Depression Inventory (BDI), Hamilton Depression Rating Scale (HAM-D), and Snaith-Hamilton Pleasure Rating Scale (SHAPS) were also administered. As detailed previously (Ballard et al., 2018), individual items from these scales, and their trajectories across treatment conditions, were used in an exploratory factor analysis to produce eight factors: depressed mood, tension, negative cognition, impaired sleep, suicidal thoughts, reduced appetite, anhedonia, and amotivation. Because not all participants completed the SHAPS, data for the anhedonia

factor were not available for all participants and this factor was thus not considered in the current analysis. The two somatic factors, reduced appetite and impaired sleep, were also excluded as we wished to focus this investigation on cognitive and emotional symptomatology.

2.3. Data acquisition

MEG scans were acquired as previously described (Nugent et al., 2019). Briefly, one or two resting-state recordings were acquired on a 275 channel CTF system (Coquitlam, BC, Canada) at 1200 Hz with third-order synthetic gradient balancing while participants were instructed to relax with their eyes closed and to remain awake and still. Scans were 250 s in length and acquired in a seated position. Resting-state recordings were acquired at the beginning and end of the recording session, with the intention that all participants would have two recordings in case one had to be discarded later due to artifacts or movement. Because the second recording was collected for redundancy, it was placed at the end of the recording session in case a scan had to be dropped due to time constraints. Thus, all participants had either one or two recordings (some were discarded due to artifacts, as described later). T_1 weighted MRI scans were acquired on a GE scanner to provide spatial localization information. All images were visually inspected to identify and remove those with severe and pervasive artifacts.

2.4. MRI pre-processing

In order to minimize problems related to multiple comparisons during the processing of connectivity matrices, a series of 34 regions of interest (ROIs) were identified from the literature *a priori* as coordinates. These regions were chosen as the primary nodes in the DMN, SN, and CEN. Subcortical nodes (bilateral thalamus, hippocampus, and amygdala), depression-focused areas (pregenual anterior cingulate cortex (pgACC) and sgACC), and medial and bilateral orbitofrontal cortex (OFC) were also included. Finally, regions from motor and visual systems were also included, given that prior MEG AEC studies found strong connectivity within these networks (Brookes et al., 2011). A list of all regions and their coordinates appears in Table 2. MRI images were transformed to Talairach space to create 7.5 mm spherical ROIs for each node for each participant.

In order to facillitate MRI and MEG co-registration, three fiducial points (above the nasion and left and right *peri*-auricular points) were manually marked on the MRI and adjusted so that the inter-fiducial distances were equivalent. MRI images were then transformed to Talairach space using the @auto_tlrc command from the AFNI software suite (Analysis of Functional NeuroImages, NIMH, NIH, Bethesda, MD). Each of the 34 ROIs was then transformed to the participant's native MRI space using the Talairach transform derived from @auto_tlrc and the transform from the original MRI to MEG space (generated using 3dTagalign).

2.5. MEG data analysis

Following initial filtering to remove low frequency artifacts and electrical line noise, an independent components analysis (ICA) was performed using MNE-Python (Martinos Center, Massachusetts General Hospital, Boston, MA) and the pyctf toolbox (https://github.com/hyperbolicTom/pyctf). A semi-automated routine was used to flag components likely related to eye movement or cardiac artifacts, but all components were visually inspected. Any component appearing to be related to eye movement, ballistocardiogram, muscular, or other non-neural artifacts was selected for removal. Recordings with 10 or more problematic components were removed from further analysis. This threshold, while somewhat arbitrary, nevertheless represented a reasonable threshold for rejecting datasets of particularly low quality. Following inspection of all ICA decompositions, new datasets were created with artifactual components removed.

Spatial localization was performed using synthetic aperture magnetometry (Robinson and Vrba, 1999) and a multisphere headmodel. First, a covariance matrix was calculated using a broad band (2–100 Hz). Following the ICA and artifactual component removal, the MEG data was of reduced rank. Thus, a pseudo-inverse was used to calculate the beamformer weights (which necessitates inversion of the covariance matrix), and matrices were truncated to remove the 10 least significant eigenvectors. A regularization parameter equal to a factor of four times the estimated noise at each sensor was also used to augment the covariance matrix. The orientation of the source within each voxel was determined as the direction that maximized power. Depth correction was not performed as we were interested only in correlations, which were unaffected by signal magnitude.

The approach utilized herein largely followed methods established by Brookes and colleagues (Brookes et al., 2016). For each ROI, the time series projected into source space was calculated for each voxel in the ROI, weighted according to the distance from the center, and averaged. The data from each ROI were then filtered for the canonical bands: delta (2–4 Hz), theta (4–8 Hz), alpha (8–14 Hz), beta (14–30 Hz), and gamma (30–55 Hz), with filter order and transition widths calculated as in the EEGLAB routine eegfilt.m. While a higher gamma band was originally investigated, connectivity values were too small to reflect meaningful differences between groups. In addition, an "artifact gamma" time series was calculated and bandpass filtered at 200–235 Hz, presumably above brain activity. Within each frequency band, the 34 ROI time series were symmetrically orthogonalized according to methods established by Colclough and colleagues (Colclough et al., 2015) in order to minimize the effects of signal leakage on the connectivity measures. The Hilbert envelope was then calculated, smoothed (using a simple boxcar function), and decimated to 1 Hz. The Hilbert envelope "artifact gamma" time series was also calculated, smoothed, and decimated. This time series was used to approximate any artifactual gamma power related to ambient muscle tension, which may influence the physiological gamma signal. Thus, a linear least-squares regression was performed in an attempt to remove the artifactual effects from the gamma time series. As an additional step for assessing gamma band activity, any spikes (activity greater than 10 times the standard deviation) in the time series that remained after regression were removed and neighboring data interpolated. These methods were explored in detail in the supplemental materials of a previous publication (Nugent et al., 2017).

Finally, after all preprocessing on the individual ROI time series, pairwise correlation matrices were formed between ROIs both within each frequency band (e.g. theta-to-theta amplitude connectivity) as well as between frequency bands (e.g. theta-to-alpha amplitude connectivity). These were then arrayed in a "super-adjacency" matrix, as in (Brookes et al., 2016); each sub-matrix in the super-adjacency matrix is referred to as a "tile" (i.e. the theta-alpha tile represents correlations between the theta band and alpha band ROI timeseries).

As one last quality-control step to ensure that artifacts did not unduly affect our connectivity values, for each recording the mean value across all ROIs was calculated for each intra-frequency tile (i.e. delta-delta, theta-theta, etc). In addition, the mean "artifact gamma" time series was calculated across all ROIs. The mean and standard deviation of these measures was then calculated across all recordings from all participants and sessions. Any recording that exhibited intra-frequency tile mean values or mean "artifact gamma" values greater than four standard deviations above the grand mean was withdrawn from further analysis. In practice, increased theta-theta correlations generally reflect artifactual connectivity due to residual eye movements (which may be present despite removal of all ICA components that appeared related to eye movements), while increased gamma-gamma correlations or artifact gamma correlations reflect artifactual connectivity due to muscular activity.

2.6. Statistical data analysis

The resulting super-adjacency matrices were converted to two-dimensional images and analyzed using a linear mixed-effects model using 3dLME within AFNI. All models used age and gender as covariates, modeled as main effects only. In addition, if participants had two usable recordings in the baseline session, both were entered into the mixed model and coded to indicate whether the scan occurred at the beginning or end of the session. The first mixed model investigated any baseline differences between HCs and MDD participants. In addition, mixed models were also performed in SPSS to test the difference in mean connectivity over each tile. As in the full super-adjacency analysis, age and gender were covariates, modeled as main effects, and scan order was a repeated measure. Unstructured covariance matrices were used.

Following the group analysis, a second statistical model was constructed to discern which, if any, clinical measures were related to MEG connectivity in the MDD group alone. The clinical measures were previously published factor scores, (Ballard et al., 2018) as described above (see section on rating scales). Factor scores for depressed mood, tension, negative cognition, suicidal thoughts, and amotivation were included in this analysis. With the exception of diagnostic group, all the factors included in the previous mixed model were included in the present analysis. Post-hoc *t*-tests of the main effect of the factor score on connectivity were also examined. Finally, a post-hoc analysis comparing HCs and MDD participants, dichotomized by a median split of the factor score, was performed for any behavioral factors that showed a significant relationship with MEG connectivity. Correction for multiple comparisons was performed using false discovery rate, with a threshold of $q = 0.005$. This threshold was chosen to lie well below a Bonferroni correction over the five behavioral factor scores.

3. Results

3.1. Participants

Seventy-six recordings from 29 participants with MDD and 25 HCs underwent artifact removal using an ICA (each participant had up to two recordings). Three recordings were eliminated because there were more than 10 artifactual components, resulting in the removal of one MDD participant. Following the final quality analysis based on connectivity outliers, five further recordings were eliminated, which resulted in the removal of one HC and one participant with MDD. Thus, the final dataset included 27 participants with MDD and 24 HCs. Demographic information appears in Table 1.

3.2. Group comparison

No significant differences were observed in HC versus MDD participants following false discovery rate (FDR) correction for multiple comparisons over the entire super-adjacency matrix. For the within-frequency tiles, participants with MDD generally showed increased delta and theta band connectivity and reduced alpha and beta band connectivity (Fig. 1).

For the cross-frequency coupling tiles, participants with MDD showed nominally increased delta-theta, delta-alpha, and delta-beta connectivity compared to HCs. Group differences in average connectivity across all nodes was not significant for any tile. Given that the pattern of differences appeared to potentially involve a relative slowing of connectivity in MDD participants, we explored whether nodes exhibiting increased within-frequency delta or theta connectivity corresponded to nodes showing decreased within-frequency alpha or beta connectivity. A significant correlation was observed across node pairs between connectivity differences in theta band and connectivity differences in both alpha ($R = -0.26$, $p = 5.2e\text{-}10$) and beta ($R = -0.18$, $p = 1.2e\text{-}5$) bands. Thus, the same connections that showed increased theta band connectivity in MDD also tended to show reduced alpha and beta band connectivity compared to HCs (Fig. 2). The mixed model analysis was repeated to test the ratios of mean within-frequency delta and theta connectivity to within-frequency alpha and beta connectivity; significant differences were noted between HCs and MDD participants for all four ratios (delta/alpha: $F(1,47) = 6.934$, $p = 0.011$; delta/beta: $F(1,48) = 6.332$, $p = 0.015$; theta/alpha: $F(1,47) = 7.200$, $p = 0.010$; theta/beta: $F(1,47) = 7.630$, $p = 0.008$).

Table 1
Demographic information for participants included in the final analysis.

	MDD	HC
N	27	24
Age	36.6 (9.95)	34.3 (10.66)
% Female	62.96	66.67
MADRS	33.2 (4.98)	

MDD: major depressive disorder; HC: healthy control; MADRS: Montgomery-Asberg Depression Rating Scale.

Table 2
Talairach coordinates for all 34 nodes included in the adjacency matrices. Regions of interest (ROIs) are grouped together in clusters, and abbreviations used in the figures of the matrices are given.

Network/Group	Node	Abbreviation	X	Y	Z
Default Mode (DMN)	Posterior Cingulate	PostCing	0	−50	20
	amPFC	amPFC	0	54	22
	L angular gyrus	RAngGy	−49	−60	33
	R angular gyrus	LAngGy	43	−63	31
Central Executive (CEN)	LDLPFC	LDLPFC	−31	42	28
	RDLPFC	RDLPFC	35	44	28
	dmPFC	dmPFC	0	25	41
	L superior parietal	LSupPar	−44	−47	44
	R superior parietal	RSupPar	44	−47	44
Salience (SN)	dorsal cingulate	DorCing	0	24	23
	L Anterior Insula	LAI	−41	−3	6
	R Anterior Insula	RAI	41	−3	6
Subcortical	L Thalamus	LThal	−7	−12	10
	R Thalamus	RThal	7	−12	10
	L Hippocampus	LHipp	−28	−15	−14
	R Hippocampus	RHipp	28	−15	−14
	L Amygdala	LAmyg	–22	−2	−15
	R Amygdala	RAmyg	22	−2	−15
Depression-related	pgACC (rostral)	pgACC	0	38	8
	sgACC (subcollosal)	sgACC	0	23	−6
	Medial Orbitofrontal	MedOrb	0	43	−11
	L Additional Orbitofrontal	Lorb	–22	37	−12
	R Additional Orbitofrontal	Rorb	22	37	−12
Visual	L MOC	LMOC	−27	−88	0
	R MOC	RMOC	27	−88	0
	L Calcarine	Lcal	−15	−64	8
	R Calcarine	Rcal	15	−64	8
	L V1	LV1	−7	−80	2
	R V1	RV1	7	−80	2
Motor	L Primary Motor	LPrimMot	−38	–23	46
	R Primary Motor	RPrimMot	38	–23	46
	L Precentral	LPctrl	−53	−6	27
	R Precentral	RPctrl	53	−6	27
	SMA	SMA	0	−18	48

R: right; L: left; amPFC: anteromedial prefrontal cortex; dmPFC: dorsomedial prefrontal cortex; DLPFC: dorsolateral prefrontal cortex; pgACC: pregenual anterior cingulate cortex; sgACC: subgenual anterior cingulate cortex; MOC: middle occipital cortex; V1: primary visual cortex; SMA: supplementary motor area.

3.3. Connectivity correlates of behavioral factors in MDD

The primary findings concerned the relationship between

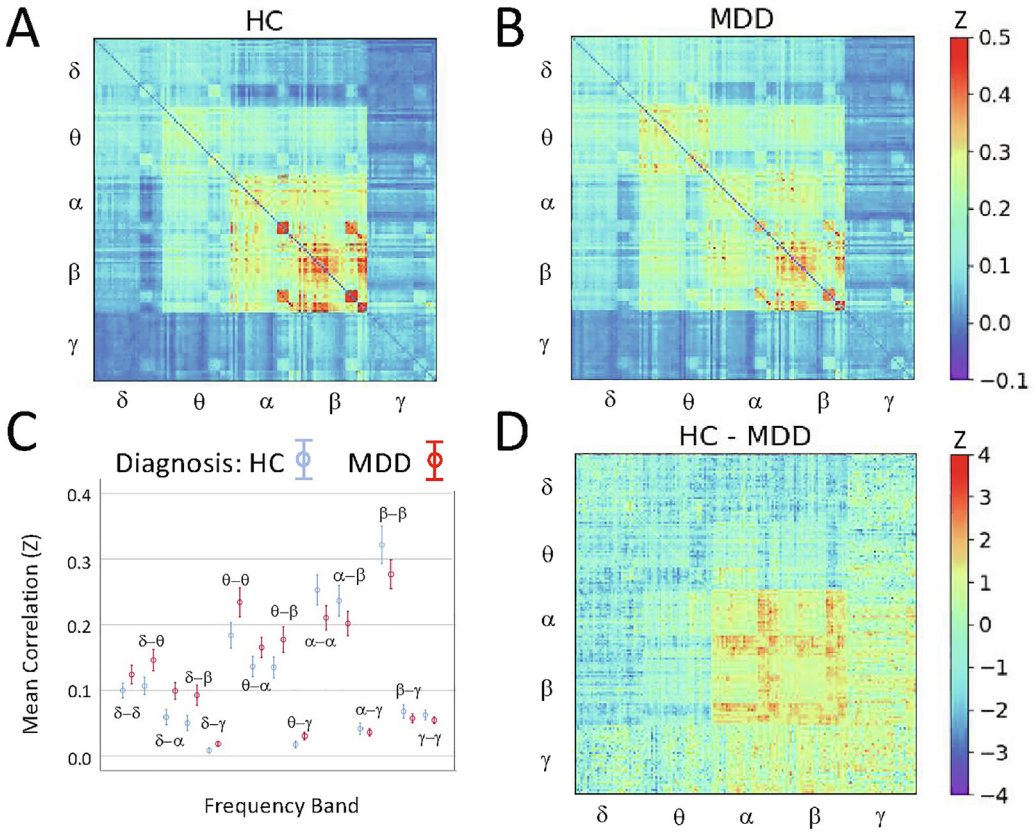

Fig. 1. Super-adjacency matrices illustrating mean connectivity in A) healthy controls (HCs) and B) participants with major depressive disorder (MDD). The raw correlation matrices were converted using the Fisher r-to-z transform before averaging. C) Mean connectivity, with standard error, for each tile in both groups. D) Z-value for the difference between HC and MDD participants.

connectivity and the suicidal thoughts/ideation (ST) factor. Due to the large number of connections surviving the initial FDR corrected threshold of $q < 0.005$, the threshold was further reduced to $q < 0.00005$ to show only the most salient connections; this corresponds to $Z \geq 4.45$. To demonstrate that the relationship between connectivity and ST may potentially reflect global dysfunction, the raw mean connectivity for significant tiles versus the ST factor was plotted in Supplemental Fig. S2, along with Pearson correlations. Supplemental Fig. S3 is a histogram illustrating the distribution of Z scores for the association between ST and connectivity across all entries in the superadjacency matrix, along with a similar plot for the relationship between connectivity and negative cognitions as a comparison. Fig. 3 shows the full super-adjacency matrix, masked such that only above-threshold connections showing a significant association with ST factor are colored. For all significant connections, higher connectivity was associated with increased suicidal ideation. Notably, in Fig. 3, the tiles showing significant positive correlations with ST factor were tiles in which mean connectivity was nominally greater in MDD participants, although the pattern of nodes involved differed.

Significant within-frequency band connections are visualized using both matrices and glass brains in Figs. 4 and 5 for delta and theta bands, respectively. Only one alpha band connection and no beta or gamma

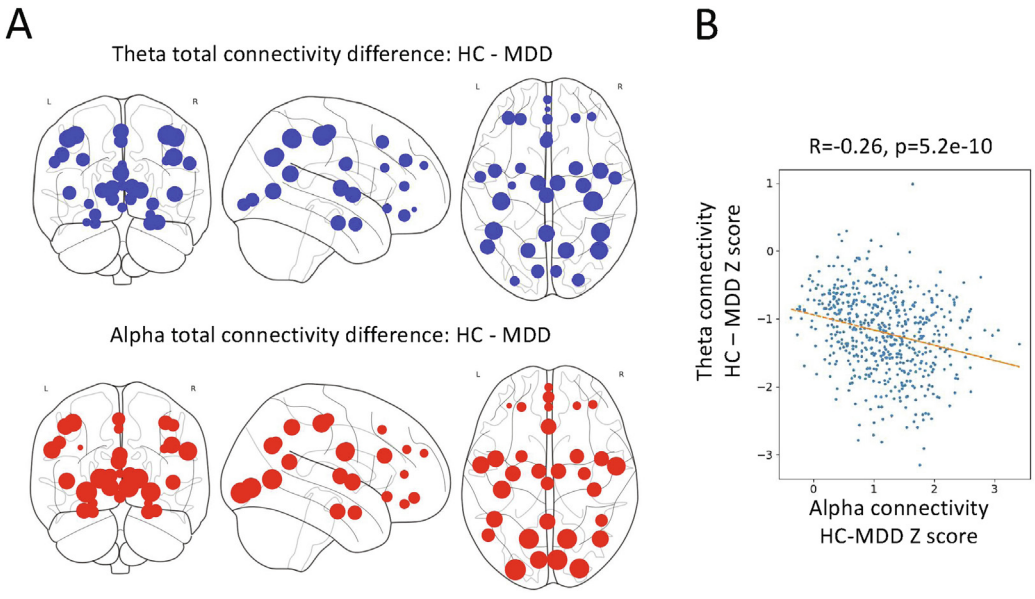

Fig. 2. A) As an aid to visualization, the total connectivity for each node was calculated as a summation of adjacency matrix along one axis for the healthy control (HC) and major depressive disorder (MDD) groups separately, and then subtracted. The size of each thus represents the difference in total connectivity of that node between groups for within-frequency theta connectivity (top) and within-frequency alpha connectivity (bottom). B) The Z-score for the difference in total theta connectivity between groups for each node pair is plotted versus the difference in total alpha connectivity, indicating that nodes showing the greatest increase in theta-mediated connectivity tended to show the greatest decrease in alpha-mediated connectivity in participants with MDD compared to HCs.

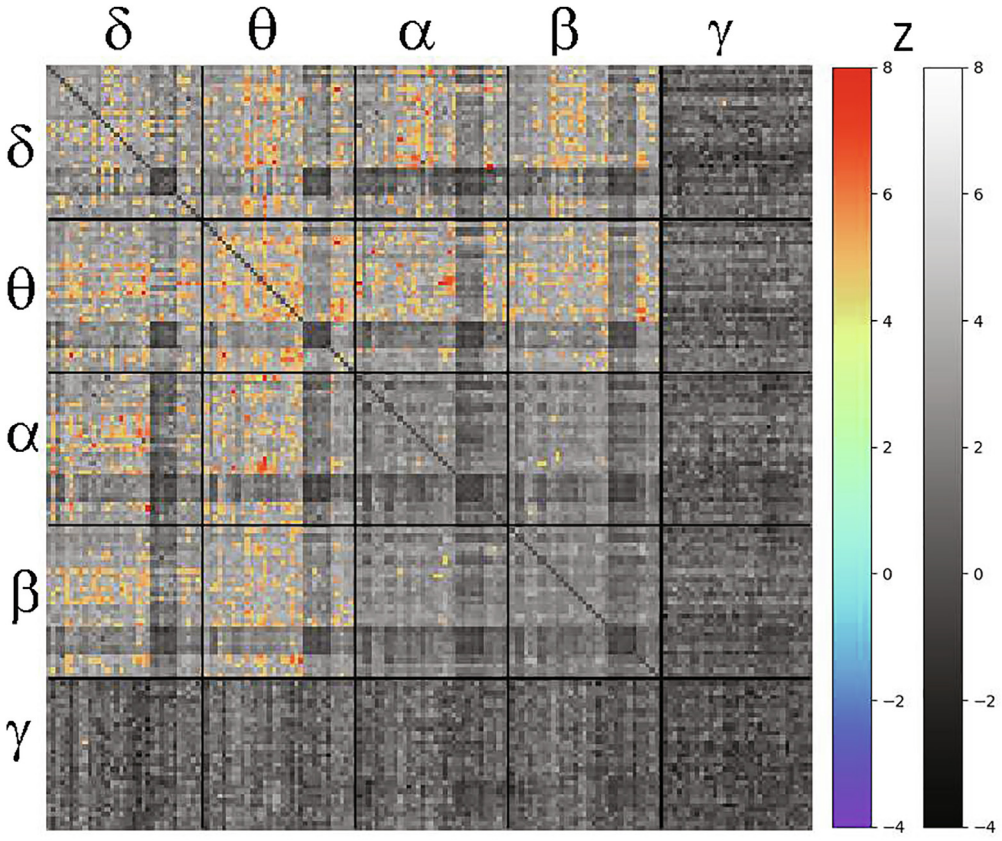

Fig. 3. Super-adjacency matrix showing Z-values for the association between connectivity and the magnitude of suicidal thoughts. Supra-threshold (Z = 4.45, q < 0.00005) connections are shown in color, and all other connections are shown in greyscale. Tiles across the diagonal represent within-band connections, while off-diagonal tiles represent connections between frequency bands.

band connections were above the threshold. The left anterior insula (LAI) and left hippocampus showed the largest number of connections correlated with the ST factor within the delta band, and these are referred to as "hubs". For theta band connectivity, there were again several hubs, including left hippocampus, left and right DLPFC, LAI, and both medial and OFC. Interestingly, motor connectivity was also

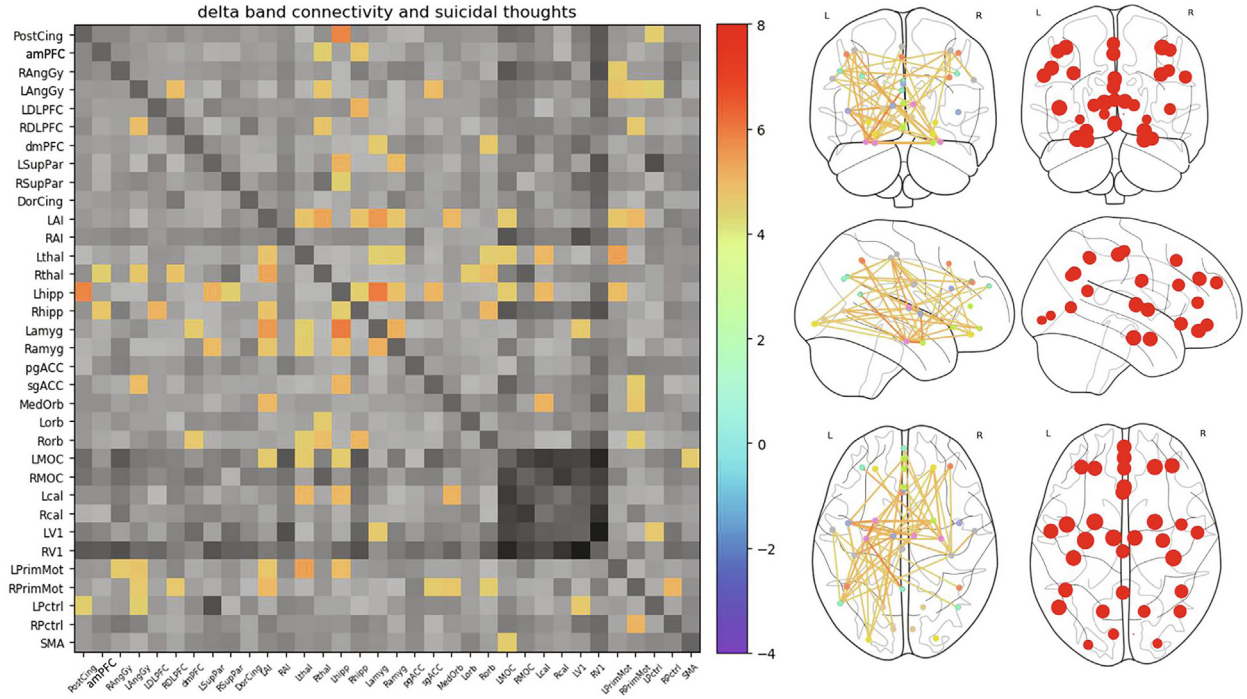

Fig. 4. Expanded delta band connectivity tile from Fig. 1 at the same statistical threshold (Z = 4.45, q < 0.00005), illustrating delta band connections significantly associated with the suicidal thoughts (ST) factor. Also shown is a glass brain perspective of the connections (middle right), as well as maps of the nodes with size scaled by the total Z value summed over all connections (far right). Left anterior insula (LAI) and left hippocampus emerged as hubs, with a large number of connections significantly associated with ST factor. Greyscale colorbar is the same as in Fig. 3, omitted here for space.

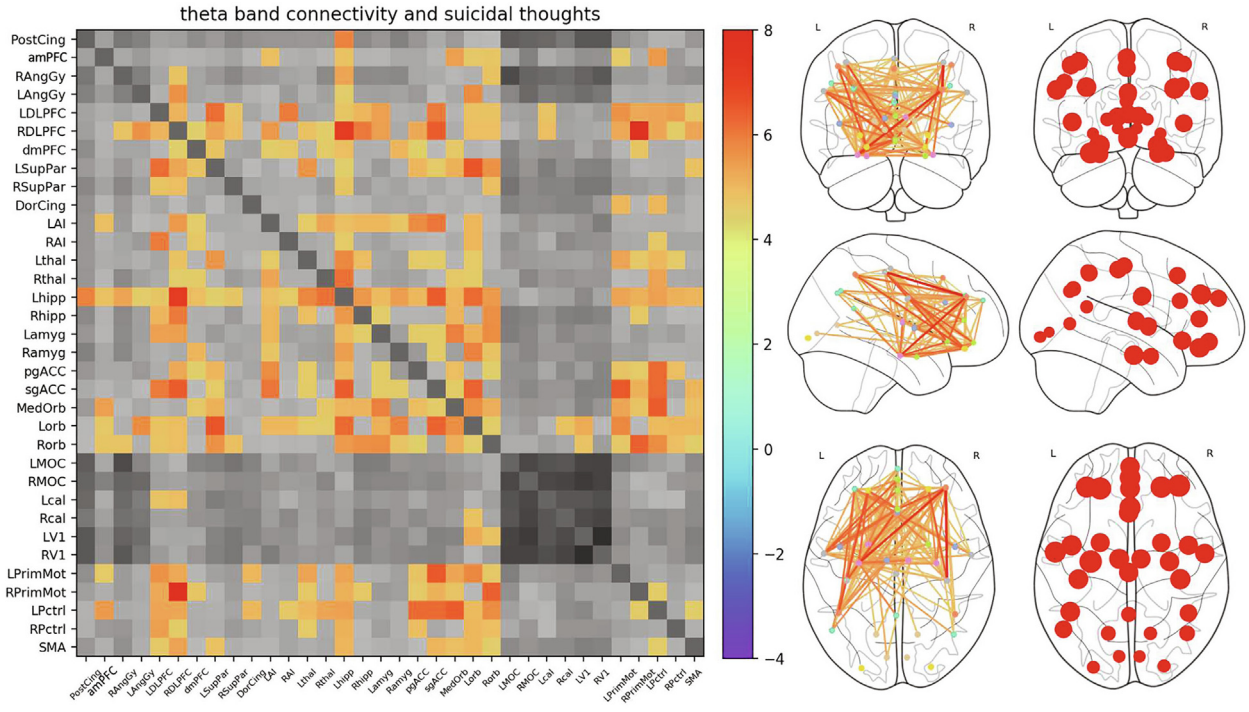

Fig. 5. Expanded theta band connectivity tile from Fig. 1 at the same statistical threshold (Z = 4.45, q < 0.00005), illustrating theta band connections significantly associated with the suicidal thoughts (ST) factor. Also shown is a glass brain perspective of the connections (middle right), as well as maps of the nodes with size scaled by the total Z value summed over all connections (far right). While anterior insula (AI) and left hippocampus still showed a large number of connections associated with the ST factor, there was greater involvement of frontal connections, particularly the left and right dorsolateral prefrontal cortex (DLPFC) and orbitofrontal regions of interest (ROIs). Greyscale colorbar is the same as in Fig. 3, omitted here for space.

prominently associated with ST factor.

Visualizing the cross-frequency connections associated with ST factor was more challenging because each cross-frequency tile is not a symmetric adjacency matrix. In order to simplify the overwhelming quantity of data, the mixed-model analysis was re-run on simplified super-adjacency matrices where the 34 regions were averaged within the respective network/group domains given in Table 1 (DMN, CEN, SN, subcortical, depression-related, visual, and motor). Fig. 6 shows the connections for delta, theta, alpha, and beta bands, thresholded to show only the 50 most significant edges (Z = 4.9, q = 3.6e-6).

A large number of delta-theta, delta-alpha, and delta-beta connections were associated with the ST factor. A significant relationship was also observed between ST factor and theta-alpha and theta-beta connections. Delta band hubs (regions showing the largest number of connections associated with the ST factor) included depression-related and subcortical ROI groups; the subcortical ROI group was also a hub in theta, alpha, and beta frequencies. The SN ROIs emerged as hubs in theta and beta frequencies. The full adjacency matrices for the individual tiles are shown in Supplemental Fig. S1. Connections involving delta band DLPFC were prominent; notably, the ST factor was related to connections between delta right DLFPC and alpha band nodes as well as to connections between delta left DLPFC and beta band nodes. ST factor was also significantly related to connections between LAI, left hippocampus, and left amygdala theta band power and delta band nodes. Correlations between alpha power in the left hippocampus and left amygdala and delta nodes were also associated with ST factor, as were correlations of beta power in LAI and left amygdala.

No connections survived the FDR-corrected q < 0.005 threshold for the depressed mood, inner tension, and amotivation factors. For the negative cognition factor, four connections survived the threshold. These likely represent type I errors due to the large number of network connections examined; nevertheless, these results are shown in Supplemental Table S1.

3.4. HCS vs. MDD participants dichotomized for suicidal thoughts

Because significant associations were observed between connection strength and ST factor scores, the MDD participant group was dichotomized by the ST factor and each subgroup was compared to the control group. Hereafter, MDD participants with high ST factor scores are referred to as the MDD_S group and those with low ST factor scores as the MDD_NS group. Because a large number of participants had an ST factor score equal to the median value, the sample size for the MDD_S group was quite small (N = 11), making these results speculative; thus, only abbreviated results are presented in the main text.

Supplemental Fig. S3 shows the super-adjacency matrices for HCs and MDD participants with low and high ST scores, as well as the Z-map for the HC vs. MDD_S group. Connectivity was greater for the MDD_S group compared to the HCs, particularly in the theta band, as well as in cross-frequency connectivity for delta-theta, delta-alpha, delta-beta, and theta-beta. For theta band connectivity, the right middle occipital cortex (MOC), RAI, and left primary motor cortex emerged as particular hubs (Fig. 7A). Connectivity was elevated in the MDD_S group in delta and theta frequencies but somewhat decreased in alpha and beta frequencies; however, there was no evidence that the same connections showing increased low frequency connectivity also showed decreased mid/high frequency connectivity.

To present the cross-frequency results, the same visualization strategy as for the behavioral factor analysis results was used, again showing only the 50 most significant network edges (Z = 3.45, q = 0.0034, Fig. 7B). Echoing the findings associated with ST factor, differences between HCs and those in the MDD_S group were most evident in delta-theta, delta-alpha, and delta-beta connectivity, along with theta-alpha and theta-beta. The most prominent hub was the delta band subcortical ROI group. As an additional confirmatory analysis, Fig. 7C shows the Z-scores from the MDD_S vs. HC analysis plotted versus the Z-scores from the within-group ST factor association analysis. Across all tiles, as well as within each tile (data not shown), the

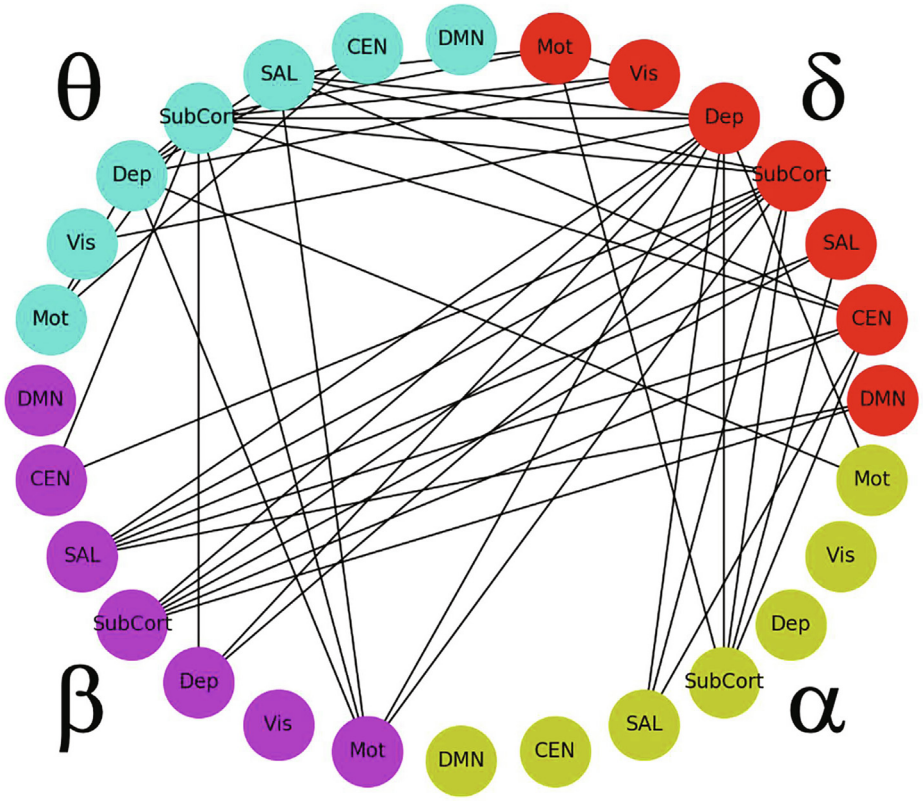

Fig. 6. Graph illustrating within- and across-frequency connections correlating with the suicidal thoughts (ST) factor, where region nodes are collapsed according to their network membership. All connections show a positive relationship with the ST factor, as in Fig. 3. The graph is thresholded to show only the 50 most significant edges for clarity (Z = 4.9, q = 3.6e-6). Abbreviations: DMN: default mode network; CEN: central executive network; SAL: salience network; SubCort: subcortical regions; Dep: depression-associated regions; Vis: visual regions; Mot: motor regions.

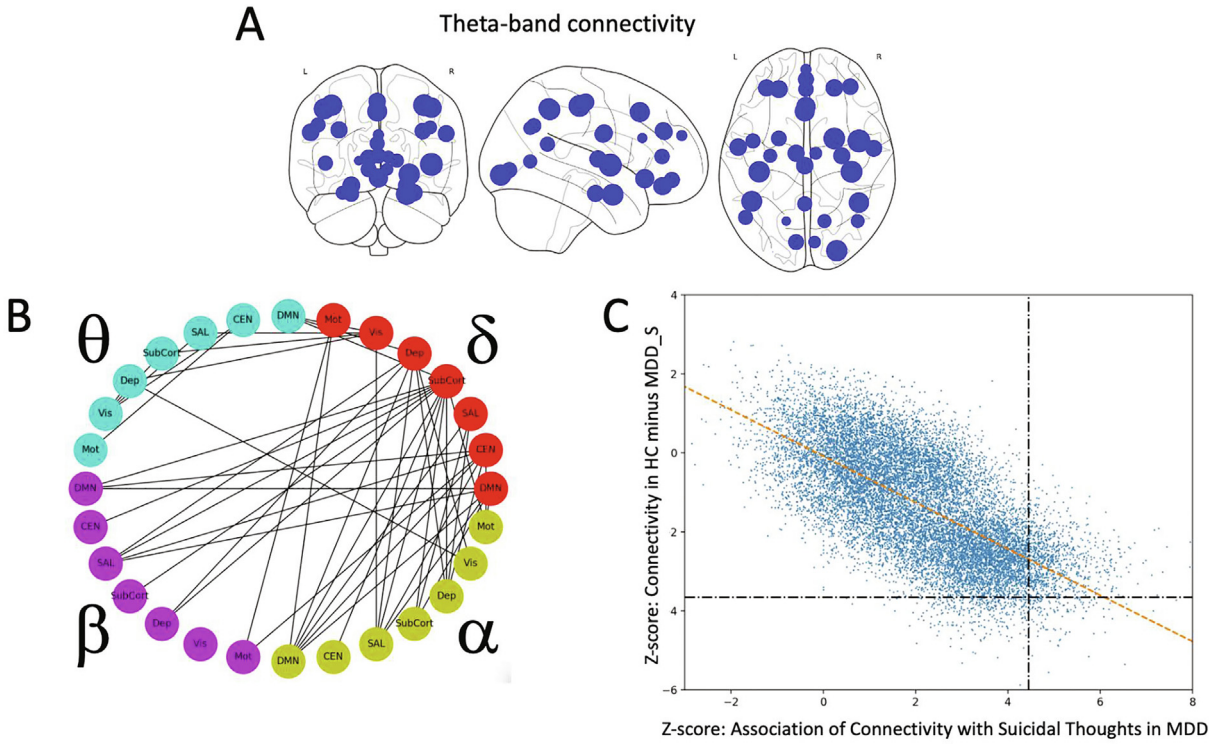

Fig. 7. A) Map of nodes with size scaled according to total Z-value for the difference between healthy controls (HCs) and individuals with major depressive disorder (MDD) with high suicidal thoughts (ST) factor scores (MDD_S). B) Within- and across-frequency connections where MDD_S participants showed greater connectivity than HCs. Regions of interest (ROIs) have been collapsed according to their network membership. The graph is thresholded to show only the 50 most significant edges for clarity (Z = 3.45, q = 0.0034). C) For all 14,365 connections in the super-adjacency matrix, the Z-score difference in connectivity between MDD_S and HC participants was plotted versus the Z-score for the association of connectivity with the magnitude of ST factor score.

connections showing the greatest difference between HCs and MDD_S participants showed the greatest correlation with ST factor in the MDD group alone (Pearson correlation $R = -0.68$). Regional differences between the MDD_S and the MDD_NS groups are not reported in the main text, given that these data are redundant with the original analysis using ST factor modeled as a continuous variable within the entire MDD group. No significant differences were observed between the HC and MDD_NS participants after FDR correction for multiple comparisons.

4. Discussion

This study is the first to investigate changes in electrophysiological connectivity between HCs and MDD participants across the frequency spectrum and to determine how connectivity in the DMN, CEN, and SN is related to symptom clusters. Two particularly salient findings emerged. First, and surprisingly, no significant differences in MEG functional connectivity were observed at baseline between HCs and individuals with MDD after correction for multiple comparisons across all connections. However, a general slowing of connectivity was noted in MDD participants, with increased delta- and theta-mediated connectivity and reduced alpha- and beta-mediated connectivity. In addition, a significant correlation was observed between connections, such that node pairs showing increased delta- and theta-mediated connectivity also showed decreased alpha- and beta-mediated connectivity. Second, and perhaps most importantly, electrophysiological connectivity was found to be strongly associated with the magnitude of suicidal thoughts in our MDD participants.

With regard to the first finding, the significance of the frequency-specific effects is unclear. Increased theta and alpha band activity have been reported in depressed individuals (reviewed in Leuchter et al., 2013), with enhanced theta rhythms hypothesized to result from aberrant generation of these rhythms in the thalamus (Schulman et al., 2011). These results are also consistent with recent findings that theta band mediated connections between subcortical and frontal nodes correlate with an array of behavioral measures (Becker and Hervais-Adelman, 2019). Fewer studies have examined connectivity in MDD across the frequency spectrum. In EEG, increased coherence was reported in multiple frequency bands (Leuchter et al., 2012), as was synchrony of transition processes in theta and alpha bands (Fingelkurts et al., 2007) and increased phase synchronization in the beta band in the DMN (Whitton et al., 2018). A recent MEG study measuring imaginary coherence observed significantly increased gamma-mediated connectivity in MDD, but no differences in any other frequency band (Jiang et al., 2019), while another study found that the likelihood of delta and theta band synchronization could be used to differentiate MDD participants from HCs (Mumtaz et al., 2018). Given the large diversity in analytic methodologies, the significance of the concordance (or discordance) of these results with ours is unclear. Using methods more similar to those employed herein, Zhang and colleagues found reduced alpha band connectivity within the DMN of MDD participants compared to controls, consistent with our findings (Zhang et al., 2018). They extended these findings by examining dynamic connectivity and found increased lifetimes for a DMN microstate in which individual nodes were negatively correlated; this finding suggests that dynamic connectivity may be a potential avenue for further research with this dataset. While it is somewhat surprising that no significant differences were observed between the HC and MDD participants, despite the strong relationship between connectivity and suicidality, this is likely accounted for by the large distribution in both ST scores and connectivity (see Supplemental Fig. S2). Notably, the MDD participants without significant ST scores largely overlapped with HC participants with regard to connectivity levels.

Perhaps our most important finding was the observation that electrophysiological connectivity was strongly associated with the magnitude of suicidal thoughts in our MDD participants. Specifically, connectivity within the delta and theta bands was associated with the presence and magnitude of the ST factor. In addition, the magnitude of the ST factor in MDD participants was associated with cross-frequency amplitude correlations for delta-theta, delta-alpha, delta-beta, theta-alpha, and theta-beta tiles. These findings were widespread, and the reported p-values were quite low, especially considering the relatively small sample size. While the strength of the finding is surprising, the additional data presented in Supplemental Figs. S2 and S3 seem to indicate that this is likely a true effect, and also likely reflects global neural dysfunction. Nevertheless, given the relatively small sample size, these results should be considered exploratory in nature.

Although the findings were widespread, several regions emerged as focused hubs in the networks associated with the ST factor, including left hippocampus, left amygdala, LAI, and bilateral DLPFC and OFC. Furthermore, the three core networks—DMN, CEN, and SN—were clearly involved; notably, the interactions between these networks most strongly associated with ST factor were primarily between- rather than within-frequency bands. Although amplitude-amplitude coupling has not been investigated as extensively as phase-amplitude coupling, it is likely that distinct neural mechanisms drive cross-frequency amplitude-amplitude coupling (reviewed in Hyafil et al., 2015), such as inhibition of gamma power by human visual oscillations to temporally segregate and prioritize components of the visual scene (Jensen et al., 2014). Evidence also exists that amplitude-amplitude coupling between low (delta or theta) and higher (alpha or beta) frequencies may be related to trait anxiety and cortisol levels (reviewed in Knyazev et al., 2019). While the underlying mechanism for this connectivity mechanism is unknown, there is speculation that it may be used for long-range neural connectivity (Bruns et al., 2000); nevertheless, the amplitude-amplitude correlation method may not be able to discern the difference between two directly connected regions and regions that are driven by a common driver.

To the best of our knowledge, only one previously published study examined suicide or suicidal ideation in MDD using MEG. Chattun and colleagues (Chattun et al., 2020) examined alpha to gamma phase amplitude coupling, or the degree to which the phase of alpha oscillations modulates the amplitude of gamma oscillations. Unmedicated participants with MDD were grouped as “high-risk” or “low-risk” based on the Nurses’ Global Assessment of Suicide Risk. Participants with MDD who were at increased risk of suicide demonstrated weaker phase amplitude coupling between the right caudate and left thalamus compared to both HCs and low-risk participants with MDD. Because phase amplitude coupling is conceptually distinct from the correlations in slow fluctuations in amplitude examined in the present study, it is difficult to comment on the convergence of these results.

Interestingly, several studies have investigated suicidal behavior and ideation using EEG. Potentially consistent with our findings of strong associations between theta band connectivity and the ST factor, Lee and colleagues found that fronto-central theta power was strongly associated with suicidal ideation in HCs with no psychiatric diagnosis (Lee et al., 2017). Several studies have investigated alpha asymmetry, finding greater left hemisphere alpha power in unmedicated suicide attempters (Graae et al., 1996; Thompson and Ong, 2018) or increases in left lateralized alpha + theta power (Iosifescu et al., 2008) associated with suicidal ideation following initiation of antidepressant treatment. However, meaningful measurements of alpha asymmetry could not be made with our data, given that laterality of power may be influenced by signal-to-noise differences due to deviations of the research participant’s head from the precise center of the MEG helmet.

Most studies examining brain connectivity and its associations with suicidal thoughts or behavior used fMRI. Although fMRI measures hemodynamic response to neuronal activity rather than directly measuring neuronal activity, consistent findings with MEG may nonetheless be observed. Several studies also employed a similar strategy of targeting triple network model nodes. In this context, reduced connectivity within the DMN, CEN, and SN has been observed to correlate with suicidal ideation (Ordaz et al., 2018), while longitudinal decreases in

ideation were associated with increased connectivity within the SN (Schwartz et al., 2019). In contrast, another study examining the DMN found increased connectivity in suicidal participants in the lingual gyrus, along with decreased connectivity in the posterior cingulate and precuneus (Zhang et al., 2016). Another study found that the dorsal anterior cingulate cortex (dACC) showed greater connectivity with a ventral posterior cingulate cortex (vPCC) than dorsal PCC (dPCC) in participants with suicidal ideation compared to HCs (Chase et al., 2017). Given that the dACC is a node of the SN, the vPCC is a core node of the DMN, and the dPCC may be associated with the CEN, this result suggests that the SN was preferentially coupled to the DMN over the CEN in participants with increased suicidal ideation. However, and in contrast to many of these results, the present study found enhanced connectivity between the three core networks in our MDD_S group, as well as positive correlations between connectivity and ST factor. Nevertheless, it is important to note that the fMRI findings are inconsistent, with no clear consensus on the direction and network location of the findings. In addition, our strongest findings involving the three core networks involved cross-frequency amplitude correlations—it is not clear how different layers in our multilayer network correlated with fMRI results, and the true relationship is likely quite complex (Tewarie et al., 2016).

A finding of particular importance is the role of the DLPFC, a key CEN node, as this region is a site for transcranial magnetic stimulation (TMS) for MDD. Preliminary evidence suggests that TMS delivered to the left DLPFC along with standard treatment may decrease the magnitude of suicidal ideation more rapidly than sham TMS and standard treatment alone (George et al., 2014). GABAergic cortical inhibition in the left DLPFC appeared to be greater in depressed adolescents with suicidal ideation (Lewis et al., 2018) and decreased following magnetic seizure therapy (MST) to a degree concomitant with the decrease in suicidal ideation (Sun et al., 2018). In addition, a high baseline index of DLPFC cortical inhibition is associated with better response to MST (Sun et al., 2016). While traditional TMS is delivered at 10 Hz (the alpha frequency), our results suggest that other frequency bands should perhaps be explored. In fact, theta-burst stimulation (TBS), which delivers pulses of 50 Hz stimulation at a frequency of 5 Hz, is also being explored as a treatment for MDD (Sonmez et al., 2019). Crucially, TBS delivered to either SN or CEN nodes may enhance connectivity within and between the three core networks (Gratton et al., 2013).

Several other fMRI studies examined suicidal ideation but did not focus solely on the triple network model. One study found that reduced connectivity in a network including the left OFC, left thalamus, and right thalamus was associated with greater suicidal ideation and behavior scores (Kim et al., 2017), while a study in psychiatric inpatients (not necessarily with MDD) showed reduced connectivity between the right AI and right OFC, but increased connectivity within the left OFC (Gosnell et al., 2019). Similarly, Weng and colleagues found reduced connectivity between the pgACC and both medial and lateral OFC and right middle temporal cortex (Du et al., 2017). In contrast, another study observed that suicide attempters showed increased connectivity between the left amygdala, right AI, and left OFC compared to non-attempters, while suicidal ideation scores were positively correlated with connectivity between the right amygdala and right parahippocampal cortex (Kang et al., 2017). This finding is consistent with other work showing increased connectivity between the bilateral amygdala and precuneus in women with MDD and suicidal ideation (Wei et al., 2018).

Unfortunately, the findings reviewed above do not converge on a single model for suicidal ideation and/or behavior. In addition, broader reviews of neuroimaging in suicide— including studies that examined more than functional connectivity—also do not converge on a circuit model. Nevertheless, the importance of several regions is clear. Specifically, studies across multiple modalities implicate the DLPFC, OFC, superior temporal cortex, AI, anterior cingulate cortex, amygdala, hippocampus, thalamus, and striatal regions (Balcioglu and Kose, 2018). Results from the present study are consistent with these, given the importance of connections involving the bilateral DLPFC, OFC, left AI, left amygdala, and left hippocampus. Interestingly, the ROIs identified as particular hubs related to ST were primarily left-lateralized. A review of the literature, however, suggests no clear laterality bias in regions involved in suicidal ideation or behavior (Balcioglu and Kose, 2018).

This manuscript has several limitations. First, our sample size was limited, particularly with regard to our comparison of HCs versus MDD participants with high ST factor scores. Due to the relatively small sample size, these results should be considered preliminary and require further validation and replication. Nevertheless, this sample of MDD participants is relatively unique in that all participants were unmedicated for at least two weeks at the time of scanning, and all had been diagnosed with treatment-resistant MDD. In addition, MDD participants were all inpatients on a well-staffed, dedicated research unit, which allowed us to enroll individuals with a wide range of suicidal ideation scores. Second, no graph analyses were performed to examine network topology or investigate interactions between layers of our multi-layer network matrices because we felt that a more straightforward analysis would be more informative as an initial examination. This analysis, conducted with stringent corrections for multiple comparisons, detected no differences between HCs and individuals with MDD, but this may be because more subtle alterations in connectivity would only be visible in overall topological properties rather than with the approach used here. Third, static functional connectivity was used; extending these methods to a dynamic realm is the subject of ongoing work.

This study is the first to examine symptom domains in MDD using MEG connectivity. While the original goal was to map heterogeneous symptom clusters onto electrophysiological connectivity, the results somewhat unexpectedly demonstrated strong associations only between connectivity and suicidal ideation. Notably, the connections associated with the ST factor involved regions known to be implicated in MDD and suicidal ideation and behavior, including the DLPFC, OFC, AI, hippocampus, and amygdala. When our MDD participants were stratified by the presence of suicidal thoughts, participants with high ST factor scores showed abnormal connectivity in similar regions to those found to be related to the magnitude of the ST factor within the MDD group. The potential identification of a biomarker for suicidal ideation could ultimately be used in treatment development and testing. In particular, these results suggest that neurostimulation, targeted at particular frequencies, might be a potential treatment for suicidal ideation in the context of MDD.

Funding

Funding for this work was supported by the Intramural Research Program at the National Institute of Mental Health, National Institutes of Health (IRP-NIMH-NIH; ZIAMH002857; NCT00088699), by a Brain and Behavior Mood Disorders Research Award to Dr. Zarate, and by a NARSAD Independent Investigator Award to Dr. Zarate. The NIMH had no further role in study design; in the collection, analysis, or interpretation of data; in the writing of the report; or in the decision to submit the paper for publication.

CRediT authorship contribution statement

Allison C. Nugent: Conceptualization, Software, Formal analysis, Data curation, Visualization, Writing - original draft. **Elizabeth D. Ballard:** Conceptualization, Writing - review & editing. **Jessica R. Gilbert:** Data curation, Formal analysis, Writing - review & editing. **Prejaas K. Tewarie:** Conceptualization, Methodology, Writing - review & editing. **Matthew J. Brookes:** Conceptualization, Methodology, Writing - review & editing. **Carlos A. Zarate:** Conceptualization, Supervision, Funding acquisition, Writing - review & editing.

Declaration of Competing Interest

Dr. Zarate is listed as a co-inventor on a patent for the use of ketamine in major depression and suicidal ideation; as a co-inventor on a patent for the use of (2R,6R)-hydroxynorketamine, (S)-dehydronorketamine, and other stereoisomeric dehydro and hydroxylated metabolites of (R,S)-ketamine metabolites in the treatment of depression and neuropathic pain; and as a co-inventor on a patent application for the use of (2R,6R)-hydroxynorketamine and (2S,6S)-hydroxynorketamine in the treatment of depression, anxiety, anhedonia, suicidal ideation, and post-traumatic stress disorders. He has assigned his patent rights to the U.S. government but will share a percentage of any royalties that may be received by the government. All other authors have no conflict of interest to disclose, financial or otherwise.

Acknowledgements

The authors thank the 7SE research unit and staff for their support. Ioline Henter (NIMH) provided invaluable editorial assistance.

Appendix A. Supplementary data

Supplementary data to this article can be found online at https://doi.org/10.1016/j.nicl.2020.102378.

References

APA, 2013. Diagnostic and Statistical Manual of Mental Disorders: Fifth Edition, DSM-5. American Psychiatric Association, Washington, DC.

Balcioglu, Y.H., Kose, S., 2018. Neural substrates of suicide and suicidal behaviour: from a neuroimaging perspective. Psychiat. Clin. Psych. 28, 314–328.

Ballard, E.D., Yarrington, J.S., Farmer, C.A., Lener, M.S., Kadriu, B., Lally, N., Williams, D., Machado-Vieira, R., Niciu, M.J., Park, L., Zarate Jr, C.A., 2018. Parsing the heterogeneity of depression: an exploratory factor analysis across commonly used depression rating scales. J. Affect. Disord. 231, 51–57.

Becker, R., Hervais-Adelman, A., 2019. Resolving the connectome — spectrally-specific functional connectivity networks and their distinct contributions to behaviour. bioRxiv. https://doi.org/10.1101/700278.

Betzel, R.F., Bassett, D.S., 2017. Multi-scale brain networks. NeuroImage 160, 73–83.

Brookes, M.J., Woolrich, M., Luckhoo, H., Price, D., Hale, J.R., Stephenson, M.C., Barnes, G.R., Smith, S.M., Morris, P.G., 2011. Investigating the electrophysiological basis of resting state networks using magnetoencephalography. Proc. Natl. Acad. Sci. 108 (40), 16783–16788.

Brookes, M.J., Tewarie, P.K., Hunt, B.A.E., Robson, S.E., Gascoyne, L.E., Liddle, E.B., Liddle, P.F., Morris, P.G., 2016. A multi-layer network approach to MEG connectivity analysis. NeuroImage 132, 425–438.

Bruns, A., Eckhorn, R., Jokeit, H., Ebner, A., 2000. Amplitude envelope correlation detects coupling among incoherent brain signals. NeuroReport 11 (7), 1509–1514.

Chase, H.W., Segreti, A.M., Keller, T.A., Cherkassky, V.L., Just, M.A., Pan, L.A., Brent, D.A., 2017. Alterations of functional connectivity and intrinsic activity within the cingulate cortex of suicidal ideators. J. Affect. Disord. 212, 78–85.

Chattun, M.R., Zhang, S., Chen, Y.u., Wang, Q., Amdanee, N., Tian, S., Lu, Q., Yao, Z., 2020. Caudothalamic dysfunction in drug-free suicidally depressed patients: an MEG study. Eur. Arch. Psychiatry Clin. Neurosci. 270 (2), 217–227.

Colclough, G.L., Brookes, M.J., Smith, S.M., Woolrich, M.W., 2015. A symmetric multivariate leakage correction for MEG connectomes. NeuroImage 117, 439–448.

De Domenico, M., 2017. Multilayer modeling and analysis of human brain networks. GigaScience 6, 1–8.

Dinga, R., Schmaal, L., Penninx, B.W.J.H., van Tol, M.J., Veltman, D.J., van Velzen, L., Mennes, M., van der Wee, N.J.A., Marquand, A.F., 2019. Evaluating the evidence for biotypes of depression: methodological replication and extension of. NeuroImage: Clin. 22, 101796. https://doi.org/10.1016/j.nicl.2019.101796.

Dong, M., Zeng, L.-N., Lu, L.i., Li, X.-H., Ungvari, G.S., Ng, C.H., Chow, I.H.I., Zhang, L., Zhou, Y., Xiang, Y.-T., 2019. Prevalence of suicide attempt in individuals with major depressive disorder: a meta-analysis of observational surveys. Psychol. Med. 49 (10), 1691–1704.

Drevets, W.C., Price, J.L., Furey, M.L., 2008. Brain structural and functional abnormalities in mood disorders: implications for neurocircuitry models of depression. Brain Struct. Funct. 213 (1-2), 93–118.

Drysdale, A.T., Grosenick, L., Downar, J., Dunlop, K., Mansouri, F., Meng, Y., Fetcho, R.N., Zebley, B., Oathes, D.J., Etkin, A., Schatzberg, A.F., Sudheimer, K., Keller, J., Mayberg, H.S., Gunning, F.M., Alexopoulos, G.S., Fox, M.D., Pascual-Leone, A., Voss, H.U., Casey, B.J., Dubin, M.J., Liston, C., 2017. Resting-state connectivity biomarkers define neurophysiological subtypes of depression. Nat. Med. 23 (1), 28–38.

Du, L., Zeng, J., Liu, H., Tang, D., Meng, H., Li, Y., Fu, Y., 2017. Fronto-limbic disconnection in depressed patients with suicidal ideation: a resting-state functional connectivity study. J. Affect. Disord. 215, 213–217.

Evans, J.W., Szczepanik, J., Brutsché, N., Park, L.T., Nugent, A.C., Zarate Jr., C.A., 2018. Default mode connectivity in major depressive disorder measured up to 10 days after ketamine administration. Biol. Psychiatry 84 (8), 582–590.

Feder, S., Sundermann, B., Wersching, H., Teuber, A., Kugel, H., Teismann, H., Heindel, W., Berger, K., Pfleiderer, B., 2017. Sample heterogeneity in unipolar depression as assessed by functional connectivity analyses is dominated by general disease effects. J. Affect. Disord. 222, 79–87.

Fingelkurts, A.A., Fingelkurts, A.A., Rytsälä, H., Suominen, K., Isometsä, E., Kähkönen, S., 2007. Impaired functional connectivity at EEG alpha and theta frequency bands in major depression. Hum. Brain Mapp. 28 (3), 247–261.

George, M.S., Raman, R., Benedek, D.M., Pelic, C.G., Grammer, G.G., Stokes, K.T., Schmidt, M., Spiegel, C., DeAlmeida, N., Beaver, K.L., Borckardt, J.J., Sun, X., Jain, S., Stein, M.B., 2014. A two-site pilot randomized 3 day trial of high dose left prefrontal repetitive transcranial magnetic stimulation (rTMS) for suicidal inpatients. Brain Stimul. 7 (3), 421–431.

Gosnell, S.N., Fowler, J.C., Salas, R., 2019. Classifying suicidal behavior with resting-state functional connectivity and structural neuroimaging. Acta Psychiatr. Scand. 140 (1), 20–29.

Graae, F., Tenke, C., Bruder, G., Rotheram, M.-J., Piacentini, J., Castro-Blanco, D., Leite, P., Towey, J., 1996. Abnormality of EEG alpha asymmetry in female adolescent suicide attempters. Biol. Psychiatry 40 (8), 706–713.

Gratton, C., Lee, T.G., Nomura, E.M., et al., 2013. The effect of theta-burst TMS on cognitive control networks measured with resting state fMRI. Front. Syst. Neurosci. 7, 124.

Greicius, M.D., Flores, B.H., Menon, V., Glover, G.H., Solvason, H.B., Kenna, H., Reiss, A.L., Schatzberg, A.F., 2007. Resting-state functional connectivity in major depression: abnormally increased contributions from subgenual cingulate cortex and thalamus. Biol. Psychiatry 62 (5), 429–437.

Groenewold, N.A., Opmeer, E.M., de Jonge, P., Aleman, A., Costafreda, S.G., 2013. Emotional valence modulates brain functional abnormalities in depression: evidence from a meta-analysis of fMRI studies. Neurosci. Biobehav. Rev. 37 (2), 152–163.

Guo, C.C., Hyett, M.P., Nguyen, V.T., Parker, G.B., Breakspear, M.J., 2016. Distinct neurobiological signatures of brain connectivity in depression subtypes during natural viewing of emotionally salient films. Psychol. Med. 46 (7), 1535–1545.

Hamilton, J.P., Etkin, A., Furman, D.J., Lemus, M.G., Johnson, R.F., Gotlib, I.H., 2012. Functional neuroimaging of major depressive disorder: a meta-analysis and new integration of baseline activation and neural response data. AJP 169 (7), 693–703.

Hyafil, A., Giraud, A.-L., Fontolan, L., Gutkin, B., 2015. Neural cross-frequency coupling: connecting architectures, mechanisms, and functions. Trends Neurosci. 38 (11), 725–740.

Hyett, M.P., Parker, G.B., Guo, C.C., Zalesky, A., Nguyen, V.T., Yuen, T., Breakspear, M., 2015. Scene unseen: disrupted neuronal adaptation in melancholia during emotional film viewing. NeuroImage: Clin. 9, 660–667.

Insel, T., Cuthbert, B., Garvey, M., Heinssen, R., Pine, D.S., Quinn, K., Sanislow, C., Wang, P., 2010. Research domain criteria (RDoC): toward a new classification framework for research on mental disorders. AJP 167 (7), 748–751.

Iosifescu, D.V., Greenwald, S., Devlin, P., Perlis, R.H., Denninger, J.W., Alpert, J.E., Fava, M., 2008. Pretreatment frontal EEG and changes in suicidal ideation during SSRI treatment in major depressive disorder. Acta Psychiatr. Scand. 117 (4), 271–276.

Jensen, O., Gips, B., Bergmann, T.O., Bonnefond, M., 2014. Temporal coding organized by coupled alpha and gamma oscillations prioritize visual processing. Trends Neurosci. 37 (7), 357–369.

Jiang, H., Tian, S., Bi, K., Lu, Q., Yao, Z., 2019. Hyperactive frontolimbic and frontocentral resting-state gamma connectivity in major depressive disorder. J. Affect. Disord. 257, 74–82.

Kaiser, R.H., Andrews-Hanna, J.R., Wager, T.D., Pizzagalli, D.A., 2015. Large-scale network dysfunction in major depressive disorder: a meta-analysis of resting-state functional connectivity. JAMA Psychiatry 72 (6), 603. https://doi.org/10.1001/jamapsychiatry.2015.0071.

Kang, S.-G., Na, K.-S., Choi, J.-W., Kim, J.-H., Son, Y.-D., Lee, Y.J., 2017. Resting-state functional connectivity of the amygdala in suicide attempters with major depressive disorder. Prog. Neuro-Psychopharmacol. Biol. Psychiatry 77, 222–227.

Kim, K., Kim, S.-W., Myung, W., Han, C.E., Fava, M., Mischoulon, D., Papakostas, G.I., Seo, S.W., Cho, H., Seong, J.-K., Jeon, H.J., 2017. Reduced orbitofrontal-thalamic functional connectivity related to suicidal ideation in patients with major depressive disorder. Sci. Rep. 7 (1). https://doi.org/10.1038/s41598-017-15926-0.

Knyazev, G.G., Savostyanov, A.N., Bocharov, A.V., Aftanas, L.I., 2019. EEG cross-frequency correlations as a marker of predisposition to affective disorders. Heliyon 5 (11), e02942. https://doi.org/10.1016/j.heliyon.2019.e02942.

Lee, S.M., Jang, K.-I., Chae, J.-H., 2017. Electroencephalographic correlates of suicidal ideation in the theta band. Clin. EEG Neurosci. 48 (5), 316–321.

Leuchter, A.F., Cook, I.A., Hunter, A.M., et al., 2012. Resting-state quantitative electroencephalography reveals increased neurophysiologic connectivity in depression. PLoS One 7, e32508.

Leuchter, A.F., Cook, I.A., Jin, Y., et al., 2013. The relationship between brain oscillatory activity and therapeutic effectiveness of transcranial magnetic stimulation in the treatment of major depressive disorder. Front. Hum. Neurosci. 7, 37.

Lewis, C.P., Nakonezny, P.A., Blacker, C.J., Vande Voort, J.L., Port, J.D., Worrell, G.A., Jo, H.J., Daskalakis, Z.J., Croarkin, P.E., 2018. Cortical inhibitory markers of lifetime suicidal behavior in depressed adolescents. Neuropsychopharmacology 43 (9), 1822–1831.

Mandke, K., Meier, J., Brookes, M.J., O'Dea, R.D., Van Mieghem, P., Stam, C.J., Hillebrand, A., Tewarie, P., 2018. Comparing multilayer brain networks between groups: Introducing graph metrics and recommendations. NeuroImage 166, 371–384.

Manoliu, A., Meng, C., Brandl, F., et al., 2013. Insular dysfunction within the salience network is associated with severity of symptoms and aberrant inter-network

connectivity in major depressive disorder. Front. Hum. Neurosci. 7, 930.
Menon, V., 2011. Large-scale brain networks and psychopathology: a unifying triple network model. Trends Cogn. Sci. 15 (10), 483–506.
Montgomery, S.A., Åsberg, M., 1979. A new depression scale designed to be sensitive to change. Br. J. Psychiatry 134 (4), 382–389.
Mumtaz, W., Ali, S.S.A., Yasin, M.A.M., Malik, A.S., 2018. A machine learning framework involving EEG-based functional connectivity to diagnose major depressive disorder (MDD). Med. Biol. Eng. Comput. 56 (2), 233–246.
Nugent, A.C., Robinson, S.E., Coppola, R., Furey, M.L., Zarate Jr., C.A., 2015. Group differences in MEG-ICA derived resting state networks: application to major depressive disorder. NeuroImage 118, 1–12.
Nugent, A.C., Luber, B., Carver, F.W., et al., 2017. Deriving frequency-dependent spatial patterns in MEG-derived resing state sensorimotor network: a novel multiband ICA technique. Hum Brain Mapp 38, 779–791.
Nugent, A.C., Ballard, E.D., Gould, T.D., Park, L.T., Moaddel, R., Brutsche, N.E., Zarate Jr., C.A., 2019. Ketamine has distinct electrophysiological and behavioral effects in depressed and healthy subjects. Mol. Psychiatry 24 (7), 1040–1052.
Ordaz, S.J., Goyer, M.S., Ho, T.C., Singh, M.K., Gotlib, I.H., 2018. Network basis of suicidal ideation in depressed adolescents. J. Affect. Disord. 226, 92–99.
Pizzagalli, D.A., Oakes, T.R., Fox, A.S., Chung, M.K., Larson, C.L., Abercrombie, H.C., Schaefer, S.M., Benca, R.M., Davidson, R.J., 2004. Functional but not structural subgenual prefrontal cortex abnormalities in melancholia. Mol. Psychiatry 9 (4), 393–405.
Quinn, C.R., Rennie, C.J., Harris, A.W.F., Kemp, A.H., 2014. The impact of melancholia versus non-melancholia on resting-state, EEG alpha asymmetry: electrophysiological evidence for depression heterogeneity. Psychiatry Res. 215 (3), 614–617.
Robinson, S.E., Vrba, J., 1999. Functional Neuroimaging by Synthetic Aperture Magnetometry (SAM). Tohoku University Press, Biomag. Sendai, pp. 302–305.
Sackeim, H.A., 2001. The definition and meaning of treatment-resistant depression. J. Clin. Psychiatry 62 (Suppl 16), 10–17.
Schulman, J.J., Cancro, R., Lowe, S., et al., 2011. Imaging of thalamocortical dysrhythmia in neuropsychiatry. Front. Hum. Neurosci. 5, 69.
Schwartz, J., Ordaz, S.J., Ho, T.C., Gotlib, I.H., 2019. Longitudinal decreases in suicidal ideation are associated with increases in salience network coherence in depressed adolescents. J. Affect. Disord. 245, 545–552.
Sheline, Y.I., Barch, D.M., Price, J.L., Rundle, M.M., Vaishnavi, S.N., Snyder, A.Z., Mintun, M.A., Wang, S., Coalson, R.S., Raichle, M.E., 2009. The default mode network and self-referential processes in depression. PNAS 106 (6), 1942–1947.
Sonmez, A.I., Camsari, D.D., Nandakumar, A.L., Voort, J.L.V., Kung, S., Lewis, C.P., Croarkin, P.E., 2019. Accelerated TMS for depression: a systematic review and meta-analysis. Psychiatry Res. 273, 770–781.
Sun, Y., Farzan, F., Mulsant, B.H., Rajji, T.K., Fitzgerald, P.B., Barr, M.S., Downar, J., Wong, W., Blumberger, D.M., Daskalakis, Z.J., 2016. Indicators for remission of suicidal ideation following magnetic seizure therapy in patients with treatment-resistant depression. JAMA Psychiatry 73 (4), 337. https://doi.org/10.1001/jamapsychiatry.2015.3097.
Sun, Y., Blumberger, D.M., Mulsant, B.H., Rajji, T.K., Fitzgerald, P.B., Barr, M.S., Downar, J., Wong, W., Farzan, F., Daskalakis, Z.J., 2018. Magnetic seizure therapy reduces suicidal ideation and produces neuroplasticity in treatment-resistant depression. Transl. Psychiatry 8 (1). https://doi.org/10.1038/s41398-018-0302-8.
Tewarie, P., Hillebrand, A., van Dijk, B.W., Stam, C.J., O'Neill, G.C., Van Mieghem, P., Meier, J.M., Woolrich, M.W., Morris, P.G., Brookes, M.J., 2016. Integrating cross-frequency and within band functional networks in resting-state MEG: a multi-layer network approach. NeuroImage 142, 324–336.
Tewarie, P., Bright, M.G., Hillebrand, A., Robson, S.E., Gascoyne, L.E., Morris, P.G., Meier, J., Van Mieghem, P., Brookes, M.J., 2016. Predicting haemodynamic networks using electrophysiology: the role of non-linear and cross-frequency interactions. NeuroImage 130, 273–292.
Thompson, C., Ong, E.L.C., 2018. The association between suicidal behavior, attentional control, and frontal asymmetry. Front. Psychiatry 9, 79.
Tian, S., Chattun, M.R., Zhang, S., Bi, K., Tang, H., Yan, R., Wang, Q., Yao, Z., Lu, Q., 2019. Dynamic community structure in major depressive disorder: a resting-state MEG study. Prog. Neuro-Psychopharmacol. Biol. Psychiatry 92, 39–47.
Wang, Q., Tian, S., Tang, H., Liu, X., Yan, R., Hua, L., Shi, J., Chen, Y.u., Zhu, R., Lu, Q., Yao, Z., 2019. Identification of major depressive disorder and prediction of treatment response using functional connectivity between the prefrontal cortices and subgenual anterior cingulate: a real-world study. J. Affect. Disord. 252, 365–372.
Wang, J., Wang, Y., Wu, X., Huang, H., Jia, Y., Zhong, S., Wu, X., Zhao, L., He, Y., Huang, L.i., Huang, R., 2020b. Shared and specific functional connectivity alterations in unmedicated bipolar and major depressive disorders based on the triple-network model. Brain Imag. Behav. 14 (1), 186–199.
Wang, J., Wang, Y., Huang, H., Jia, Y., Zheng, S., Zhong, S., Chen, G., Huang, L.i., Huang, R., 2020a. Abnormal dynamic functional network connectivity in unmedicated bipolar and major depressive disorders based on the triple-network model. Psychol. Med. 50 (3), 465–474.
Wei, S., Chang, M., Zhang, R., Jiang, X., Wang, F., Tang, Y., 2018. Amygdala functional connectivity in female patients with major depressive disorder with and without suicidal ideation. Ann. Gen. Psychiatry 17 (1). https://doi.org/10.1186/s12991-018-0208-0.
Whitton, A.E., Deccy, S., Ironside, M.L., Kumar, P., Beltzer, M., Pizzagalli, D.A., 2018. Electroencephalography source functional connectivity reveals abnormal high-frequency communication among large-scale functional networks in depression. Biol. Psychiatry Cogn. Neurosci. Neuroimag. 3 (1), 50–58.
Workman, C.I., Lythe, K.E., McKie, S., Moll, J., Gethin, J.A., Deakin, J.FW., Elliott, R., Zahn, R., 2016. Subgenual cingulate–amygdala functional disconnection and vulnerability to melancholic depression. Neuropsychopharmacology 41 (8), 2082–2090.
Zhang, S., Chen, J.-M., Kuang, L.i., Cao, J., Zhang, H., Ai, M., Wang, W.o., Zhang, S.-D., Wang, S.-y., Liu, S.-J., Fang, W.-D., 2016. Association between abnormal default mode network activity and suicidality in depressed adolescents. BMC Psychiatry 16 (1). https://doi.org/10.1186/s12888-016-1047-7.
Zhang, S., Tian, S., Chattun, M.R., Tang, H., Yan, R., Bi, K., Yao, Z., Lu, Q., 2018. A supplementary functional connectivity microstate attached to the default mode network in depression revealed by resting-state magnetoencephalography. Prog. Neuro-Psychopharmacol. Biol. Psychiatry 83, 76–85.